

Controlling the carrier concentration of the high-temperature superconductor $\text{Bi}_2\text{Sr}_2\text{CaCu}_2\text{O}_{8+\delta}$ in angle-resolved photoemission spectroscopy experiments

A. D. Palczewski and Takeshi Kondo

Ames Laboratory and Department of Physics and Astronomy, Iowa State University, Ames, Iowa 50011, USA

J. S. Wen, G. Z. J. Xu, and G. Gu

Condensed Matter Physics and Materials Science Department, Brookhaven National Laboratory, Upton, New York 11973, USA

A. Kaminski

Ames Laboratory and Department of Physics and Astronomy, Iowa State University, Ames, Iowa 50011, USA

(Received 17 September 2009; revised manuscript received 16 February 2010; published 19 March 2010)

We study the variation of the electronic properties at the surface of a high-temperature superconductor as a function of vacuum conditions in angle-resolved photoemission spectroscopy experiments. Normally, under inadequate ultrahigh vacuum (UHV) conditions the carrier concentration of $\text{Bi}_2\text{Sr}_2\text{CaCu}_2\text{O}_{8+\delta}$ (Bi2212) increases with time due to the absorption of oxygen from CO_2/CO molecules that are prime contaminants present in UHV systems. We find that in an optimal vacuum environment at low temperatures, the surface of Bi2212 is quite stable (the carrier concentration remains constant); however at elevated temperatures the carrier concentration decreases due to the loss of oxygen atoms from the Bi-O layer. These two effects can be used to control the carrier concentration *in situ*. Our finding opens the possibility of studying the electronic properties of the cuprates as a function of doping across the phase diagram on the same surface of sample (i.e., with the same impurities and nondopant defects). We envision that this method could be utilized in other surface sensitive techniques such as scanning tunneling microscopy/spectroscopy.

DOI: [10.1103/PhysRevB.81.104521](https://doi.org/10.1103/PhysRevB.81.104521)

PACS number(s): 74.70.Dd, 71.18.+y, 71.20.-b, 71.27.+a

I. INTRODUCTION

Surface techniques have played an important role in understanding the properties of the high-temperature superconductors. They have revealed a number of fascinating phenomena such as the direct observation of the superconducting gap¹ and its anisotropy,^{2,3} confirmation of the *d*-wave symmetry of the order parameter, direct observation of the pseudogap and its anisotropy,⁴⁻⁶ discovery of spatial inhomogeneities,^{7,8} unusual spatial ordering,⁹ nodal quasiparticles,¹⁰ renormalization effects,¹¹⁻¹³ and many others.^{14,15} The success of these techniques rely on the fact that the layers in some cuprates are very weakly bonded via the Van der Waals interaction. In such cases the bulk properties and surface properties are essentially identical, since there is no charge exchange between the layers. The samples in such cases can be thought of as a stack of very weakly electrically coupled two-dimensional conducting surfaces rather than a three-dimensional object. Two of the most commonly studied materials with this property are $\text{Bi}_2\text{Sr}_2\text{CaCu}_2\text{O}_{8+\delta}$ (Bi2212) and $\text{Bi}_2\text{Sr}_2\text{CuO}_{6+\delta}$ (Bi2201). There is however one important aspect that needs to be carefully considered, namely the stability of the cleaved samples under ultrahigh vacuum (UHV) conditions. UHV is a rather broad term and refers to pressures lower than 1×10^{-9} Torr. Quite often such conditions are not sufficient to guarantee the stability of the surface, particularly in the case of nonstoichiometric materials such as the cuprates. These problems were recognized early on,² and subsequent measurements revealed significant changes in the electronic properties as a function of time after cleaving. This issue was not carefully examined following these first measurements,

and it is likely an important source of data discrepancies among the various groups.^{14,15}

Here we present a systematic study of the electronic properties of Bi2212 as a function of vacuum conditions. There are significant difficulties with quantifying vacuum conditions in deep UHV regime due to lack of common methods for absolute measurement partial pressure. More significantly, the main problem with quantifying the vacuum conditions lies in fact that transport at very low pressures is ballistic in nature; thus influx of molecules experienced by the sample surface and entrance of residual gas analyzer (RGA) or ion gauge may be very different. The core of vacuum problems in angle-resolved photoemission spectroscopy (ARPES) setup is electron analyzer. It is typically the worst pumped part of the system, with many layers of shielding and electron surfaces. Gases desorbed inside of the analyzer exit via electron lens and hit cold surface of the sample. Those which do not stick are most likely pumped before they get to the RGA/ion gauge. In case of our setup this problem was solved by extensive baking of the analyzer (with cumulative baking time of several months). We demonstrate that under less than ideal vacuum conditions (defined as a condition where the results of identical measurements vary with time), increased carrier concentration arises due to the breakup of CO_2/CO molecules by exposure to vacuum ultraviolet (VUV) photons and the subsequent adsorption of oxygen into the BiO layers. We demonstrate that this effect is most likely responsible for observation of bilayer splitting in Bi2212 in nominally “underdoped” samples. We show that when tiny (10^{-10} Tr level) leak is introduced to the UHV system, the carrier concentration of sample surface increases without exposure to VUV photons.

When the partial pressure of active gases is kept to optimal levels (again defined as condition, where result of measurements do not change significantly with time), the lifetime of cleaved surface of Bi2212 can be as long as a few weeks at low temperatures ($T < 150$ K). At elevated temperatures ($T > 200$ K) the sample surface loses oxygen, which results in the reduction of carrier concentration. This second effect is most likely responsible for the recently reported nonmonotonic temperature dependence of the pseudogap,¹⁶ where at elevated temperatures the sample surface becomes underdoped and therefore develops a pseudogap. We demonstrate that these two effects (*in situ* absorption and desorption of oxygen) can be utilized to control the carrier concentration of the sample surface. This approach enables one to study the intrinsic electronic properties of the cuprates across the phase diagram using a single cleave of the sample. This eliminates many extrinsic effects such as changing the chemical impurities and nondopant defects.

II. EXPERIMENTAL DETAILS

The ARPES data was acquired using a laboratory-based Scienta 2002 electron analyzer and high intensity Gamma-data UV4050 UV source with custom designed optics. The photocurrent at the sample was approximately $1 \mu\text{A}$, which corresponds to roughly 10^{13} photons/sec at 0.05% of the bandwidth. The energy resolution was set at 10 meV and momentum resolution at 0.12° and 0.5° along a direction parallel and perpendicular to the analyzer slits, respectively. Samples were mounted on a variable temperature cryostat (10–300 K) cooled by a closed cycle refrigerator. The precision of the sample positioning stage was $1 \mu\text{m}$. The partial pressure of the active gases was at the detection limit of the RGA and the pressure of hydrogen was below 3×10^{-11} Torr. Excellent vacuum conditions were achieved by strict adherence to good vacuum practices, use of UHV compatible materials, and a cumulative bake-out time of the system in excess of six months. The typical lifetime of the optimally doped Bi2212 surfaces was greater than two weeks after cleaving, defined as less than 5% change of the superconducting gap (2 meV) at 40 K. The core-level spectra were acquired on the Hermon beam-line at the Synchrotron Radiation Center using a Scienta 2002 end-station. The photon energy was set at 500 eV and energy resolution at 200 meV. The residual gas spectrum was taken by a SRS Quad Residual Gas Analyzer model RGA100 in CDEM (electron multiplier) mode, the factory stated pressure resolution is 1×10^{-13} Torr which is constant with the noise level in our data.

III. INCREASING CARRIER CONCENTRATION

It has been known for some time that aging (increased surface doping) in cuprates is caused by less than ideal UHV conditions,² that is, vacuum conditions where the spectrum is not stable as a function of time.

Aging is usually detected by measuring the superconducting gap (the energy gap as defined by the difference between the peak position of a Bi2212 spectrum and the chemical

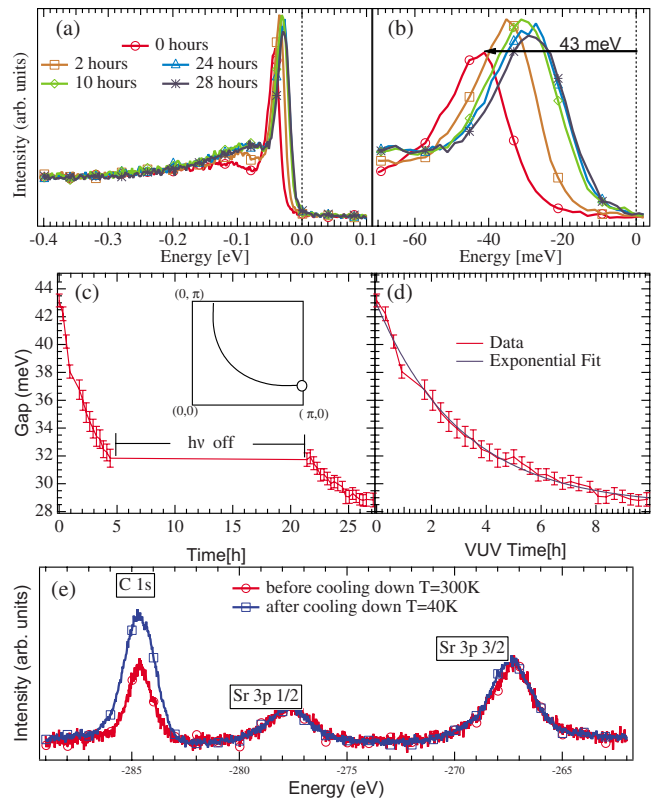


FIG. 1. (Color online) ARPES spectrum of Bi2212 taken under poor vacuum conditions (CO and CO₂ partial pressures of 8×10^{-11} Tr). (a) Sample EDC (energy distribution curves) taken at the antinode where the band crosses the Fermi energy at five different times; (b) narrow view of (a); (c) time evolution of Bi2212's superconducting gap as a function of time; (d) the time evolution of Bi2212's superconducting gap under VUV photons (red with error bars) fitted with an exponential decay (solid blue curve), the temperature for (a)–(d) was set to 20 K; (e) C 1s, Sr 3p_{1/2}, and Sr 3p_{3/2} core-level data from Bi2212, showing carbon deposits some time after cleaving and after while cooling.

potential measured by a polycrystalline gold sample) as a function of time. If the gap shifts to a lower binding energy the sample has aged.^{17,18} Figures 1(a) and 2(b) shows an example of this where a freshly cleaved Bi2212 single crystal was scanned in a less than optimal vacuum conditions to see how the spectrum changed over time. A shift to lower binding energy as well as a peak suppression was detected, showing the sample was aging. In Fig. 1(c) the size of the superconducting gap is shown as a function of time. The aging occurred only when sample surface was illuminated with VUV photons. In the absence of VUV photons on the sample, (from fifth hour to 21st hour) the aging did not progress. If consider only the time, when the sample was exposed to VUV photons, the magnitude of the gap follows an exponential decay (blue line).

In absence of leaks, a UHV system has normally undetectable levels of oxygen as measure by a residual gas attached to the ARPES system [see Fig. 2(c) red spectrum]. However in stainless steel vessels CO₂/CO are always present. These oxide molecules can adhere to clean sample surfaces especially at low temperatures. When the molecules

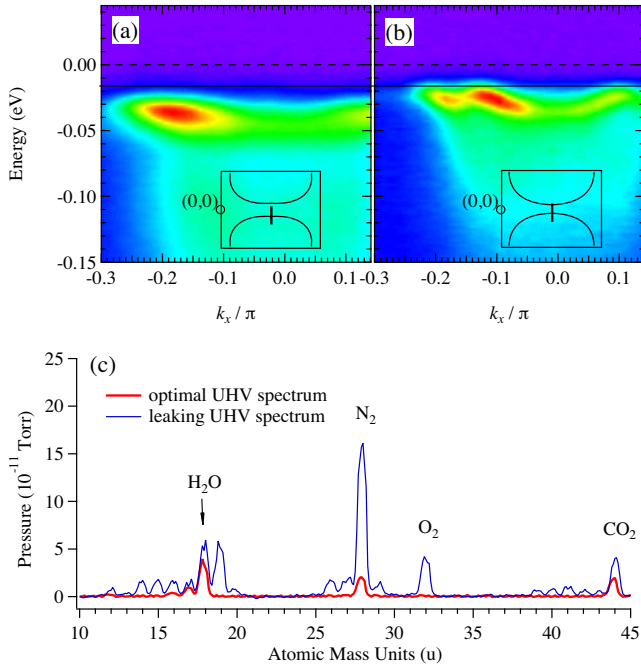


FIG. 2. (Color online) (a) ARPES intensity map of freshly cleaved optimally doped Bi2212 at $(\pi, 0)$, showing no bilayer splitting; (b) ARPES intensity maps on the same sample and the same location as in (a) only oxygen aged (*in situ* overdoing) in a UHV system with a leak for 15 h, showing bilayer splitting and a peak shift location of the Fermi momentum (the black line as a guide to the eye); (c) residual gas analyzer (RGA) spectrum after an optimal bake-out (thin red curve) and after a bake-out where there was a 10^{-10} Torr air leak (thick blue curve).

are exposed to VUV photons above 6 eV they break into carbon and oxygen;¹⁹ the oxygen can then be incorporated into BiO layer as dopant, while the carbon atoms remain on the surface. The proof of this scenario is in Fig. 1(e) where the core-level spectrum of Bi2212 at 300 and 40 K are shown. As the sample cooled more CO_2/CO molecules adhered to the surface of the sample. Since there are carbon deposits some time after cleaving and even more after cooling, it is likely the oxygen accompanied the carbon to the surface. This oxygen can then change the doping of the sample after it is dissociated from the carbon.

In the presence of a leak a UHV system can have detectable amounts of oxygen. Under these conditions a Bi2212 sample can age even without the breakdown of CO_2/CO . One of the trademarks of an overdoped (aged) Bi2212 sample is the appearance of bilayer band splitting at the antinode $(\pi, 0)$. While there has been a relatively active discussion on whether Bi2212 contains bilayer band splitting all the time or just in an overdoped state; bilayer splitting has only been seen in overdoped samples when using a helium discharge lamp.^{20–23} An example of this is shown in Fig. 2 where a fresh Bi2212 sample was scanned and then allowed to sit in the leaky UHV system overnight (15 h) before scanning again. Even though the sample was kept a 20 K, bilayer band splitting was detected after exposure for 15 h, signaling that the sample aged because of oxygen absorption. An example RGA spectrum contrasting the difference in the partial

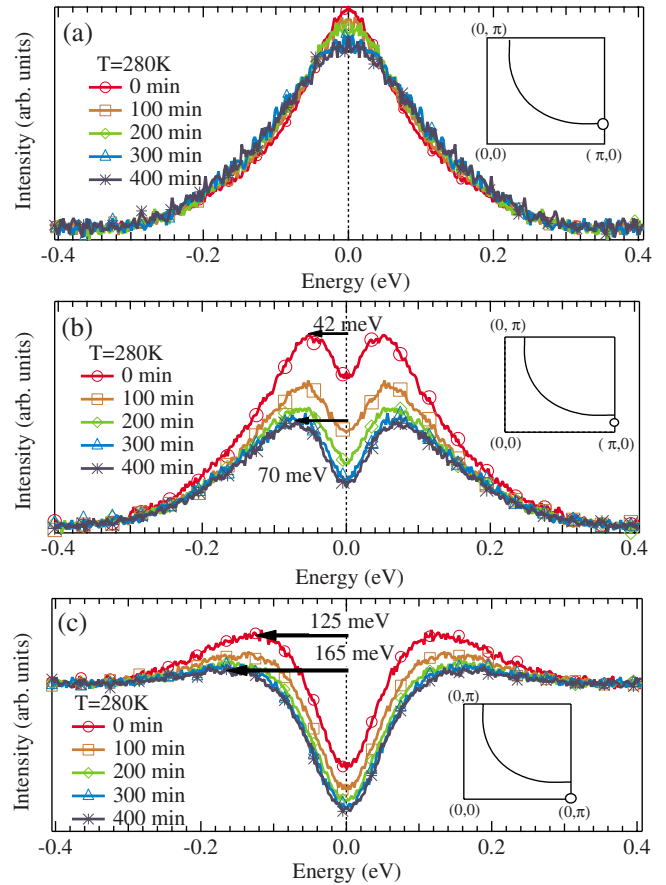


FIG. 3. (Color online) (a)–(c) symmetrized ARPES EDC's for Bi2212 taken at three points near $(\pi, 0)$, showing the time evolution of the spectrum at 280 K.

pressure of gases for an optimal UHV (red curve) and an UHV leak (blue) is shown in Fig. 2(c). The reader should notice that the leaky vacuum spectrum contains an O_2 peak absent in the optimal vacuum spectrum, as well as excess H_2O , CO_2 , and N_2/CO . We know that the vacuum contains a small air leak (10^{-10} Torr) because of the ratio of $N_2:O_2$, which is $\approx 4:1$, the same as air.

IV. DECREASING CARRIER CONCENTRATION

While in a reasonable vacuum system there can be enough CO_2/CO to change the surface doping of a sample over time; in an ultraclean UHV system samples can live for many weeks without surface degradation or a change in doping (assuming the sample is kept at low temperature). Yet, when the sample is annealed above 200K an interesting thing happens to the Bi2212's doping level; the sample doping level is reduced (the opposite of aging). This is seen in Figs. 3(a)–3(c) where the time evolution of Bi2212's EDCs at three locations at or near $(\pi, 0)$ with the sample at 280 K is shown. The sample actually changes doping moving toward lower doping (signified by a larger spectral gap). Figure 4(a) shows the energy distribution curve (EDC) at the antinodal Fermi momentum from the same sample before and after annealing at 280 K for 28 h. The superconducting gap clearly

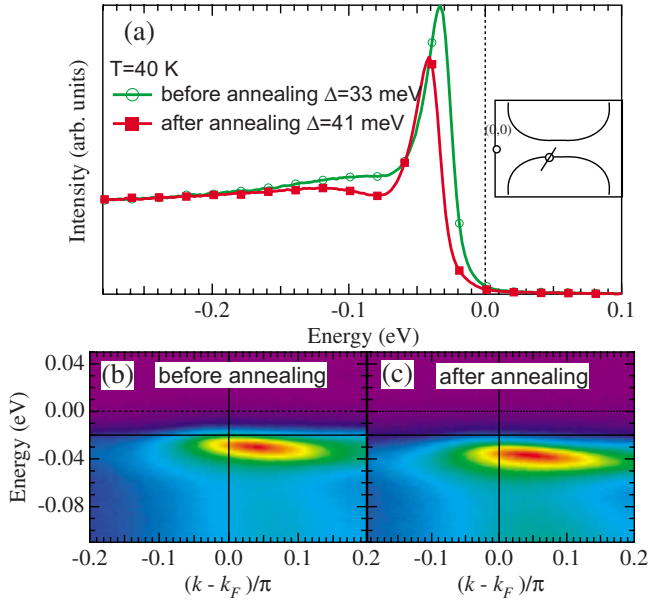


FIG. 4. (Color online) (a) EDC at the Fermi momentum close to the antinode before (green circles) and after (solid red squares) annealing at 280 K over 28 h with their respective superconducting gaps Δ ; (b)–(c) momentum intensities maps taken across Fermi momentum close to $(\pi,0)$ before and after annealing.

shifts from 33 to 41 meV and the peak is suppressed, signaling that the doping has changed from a slightly over doped sample to a more under doped sample.²⁴ The momentum color maps from Fig. 4(a) are shown in Figs. 4(b) and 4(c); after annealing the gap shifts to higher binding energy, there is also a shift in the location of the Fermi momentum. This momentum shift comes from a change in the chemical potential, which moves lower in a ridged-band-like fashion upon doping.²⁵

Another way to see if a samples carrier concentration has decreased is to look at the pseudogap. Figure 5(a) shows the EDC at the Fermi momentum before and after annealing at 280 K for 28 h. The pseudogap shifts from 30 to 50 meV. As Bi2212 goes to lower doping levels the pseudogap becomes bigger and the temperature at which the pseudogap remains (T^*) becomes higher.⁴ Figures 5(b) and 5(c) demonstrate that before annealing T^* is below 140 K with the pseudogap disappearing and after annealing T^* is above 200 K. The pseudogap transition temperature after annealing is above 200 K, which guarantees that the sample is at a lower doping level.

Until now we have only shown the lowering of doping on Bi2212 at elevated temperature. While we still have not shown if the doping change is caused by the elevated temperature or a combination of elevated temperature and VUV photons. This was tested by scanning the sample just after cleaving and again after the sample sat under UHV for 16 days at 100 K. This data is shown in Fig. 6(a). The spectrum barely changed over the two weeks. While in Fig. 6(b) we show the 280 K spectrum just after cleaving, and again after the sample sat under UHV for eight days at 280 K. Most of the spectral weight has shifted to higher binding energies and the Fermi edge has all but disappeared, signifying an almost

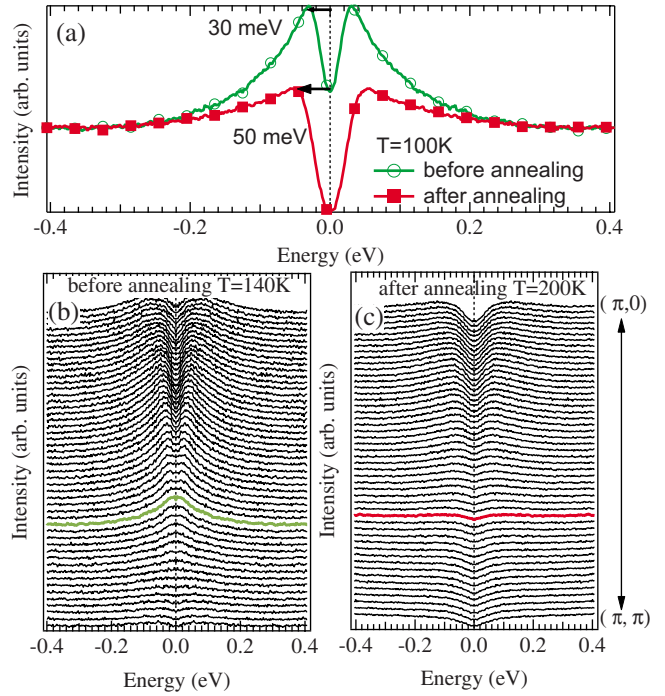


FIG. 5. (Color online) (a) 100 K symmetrized ARPES data taken at the Fermi momentum before and after annealing at 280 K for 28 h; (b) ARPES intensities at 140 K before annealing; and (c) ARPES intensities at 200 K after annealing.

completely insulating sample. From Fig. 6 we can conclude that the lowering of the samples doping is only caused by the elevated temperatures.

The greatest consequence of this study is that Bi2212's doping can be change from over doped all the way down to

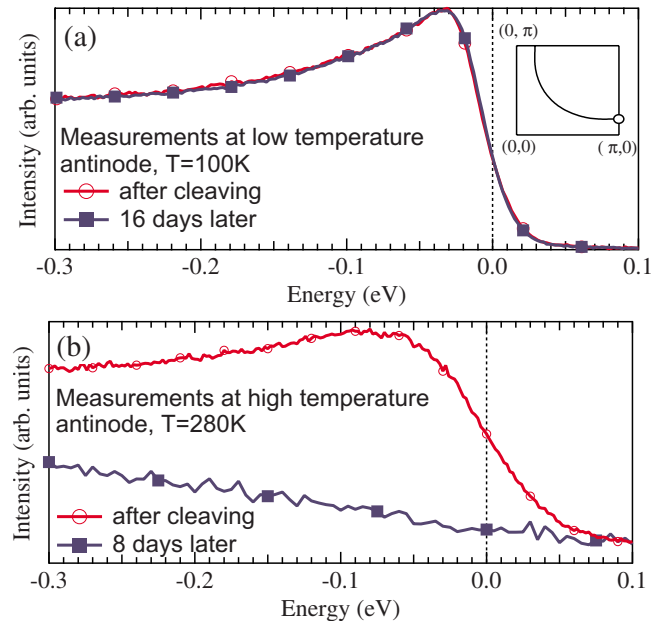


FIG. 6. (Color online) Bi2212 EDC at the Fermi momentum close to $(\pi,0)$ (a) just after cleaving at 100 K (red circles) and again after sitting at 100 K for 16 days (solid blue squares); (b) just after cleaving at 280 K (red circles) and again after sitting at 280 K for eight days (solid blue squares).

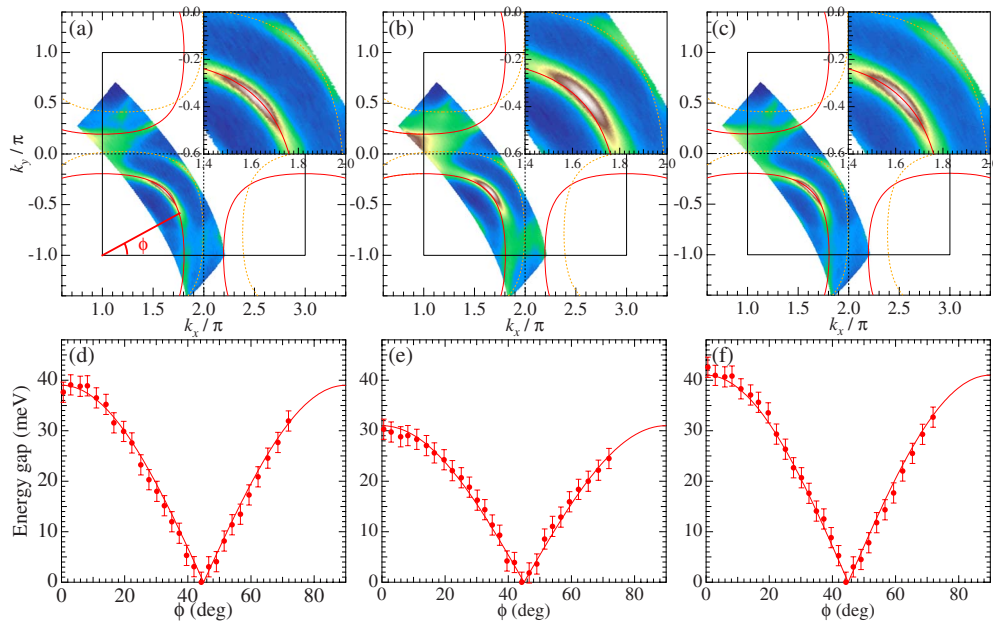


FIG. 7. (Color online) ARPES intensity plots at the Fermi energy from the same sample at three different times all at 12 K: (a) just after cleaving; (b) after a couple of days of VUV aging at low temperature; (c) after annealing at 280 K overnight; the upper right hand corner of (a)–(c) are the zoomed in images from the bottom left hand corner, the solid red and dotted yellow curves are from a tight binding fit for optimally doped Bi2212 as a guide to the eye, (d)–(f) the size of the superconducting gap as a function of angle ϕ from (a)–(c), respectively.

insulating in a systematic fashion on a single crystal. To this point the data presented has been either overdoped by aging or under doped by annealing on different samples. Figure 7 demonstrates how the same sample surface can be overdoped by aging and then underdoped by annealing to move across the phase diagram. An optimally doped Bi2212 sample was cleaved, the Fermi surface and superconducting gap values as a function of angle ϕ [angle clockwise from the line $(\pi, -\pi)$ to $(2\pi, -\pi)$] was scanned Figs. 7(a) and 7(d). Aging was detected after a couple of days of scanning Figs. 7(b) and 7(e). The sample was then annealed overnight at 280 K to remove the aging Figs. 7(c) and 7(f).

V. CONCLUSION

We have presented a systematic study of the electronic properties at the surface of Bi2212 as a function of vacuum conditions. The results confirm that under poor vacuum conditions there is an increase in carrier concentration due to the breakup of CO_2/CO molecules by exposure to vacuum ultraviolet (VUV) photons and a subsequent adsorption of oxygen into the BiO layers. We also show that with a UHV leak, where oxygen is present, a sample can increase its carrier

concentration without exposure to VUV photons. This observation confirms that bilayer splitting only occurs in overdoped Bi2212. We then show that at elevated temperatures ($T > 200$ K) the sample surface loses oxygen, which results in a reduction of the carrier concentration. These two effects (*in situ* absorption and desorption of oxygen) can be utilized to control the carrier concentration of Bi2212. This approach enables one to study the intrinsic electronic properties (i.e., without changing the impurities and nondopant defects) of the cuprates across the phase diagram in ARPES as well as other surface sensitive techniques using single cleaved surface.

ACKNOWLEDGMENTS

This work was supported by the Director's Office for Basic Energy Sciences, U.S. DOE. Work at Ames Laboratory was supported by the Department of Energy—Basic Energy Sciences under Contract No. DE-AC02-07CH11358. The work at B.N.L. was supported by Department of Energy—Basic Energy Sciences under Contract No. DE-AC02-98CH10886. Synchrotron Radiation Center is supported by the National Science Foundation under Grant No. DMR-0537588.

¹C. G. Olson, R. Liu, A.-B. Yang, D. W. Lynch, A. J. Arko, R. S. List, B. W. Veal, Y. C. Chang, P. Z. Jiang, and A. P. Paulikas, *Science* **245**, 731 (1989).

²Z.-X. Shen, D. S. Dessau, B. O. Wells, D. M. King, W. E. Spicer, A. J. Arko, D. Marshall, L. W. Lombardo, A. Kapitulnik, P.

Dickinson, S. Doniach, J. DiCarlo, A. G. Loeser, and C. H. Park, *Phys. Rev. Lett.* **70**, 1553 (1993).

³H. Ding, M. R. Norman, J. C. Campuzano, M. Randeria, A. F. Bellman, T. Yokoya, T. Takahashi, T. Mochiku, and K. Kadowaki, *Phys. Rev. B* **54**, R9678 (1996).

- ⁴H. Ding, T. Yokoya, J. C. Campuzano, T. Takahashi, M. Randeria, M. R. Norman, T. Mochiku, K. Kadowaki, and J. Giapintzakis, *Nature* (London) **382**, 51 (1996).
- ⁵A. G. Loeser, Z.-X. Shen, D. S. Dessau, D. S. Marshall, C. H. Park, P. Fournier, and A. Kapitulnik, *Science* **273**, 325 (1996).
- ⁶M. R. Norman, H. Ding, M. Randeria, J. C. Campuzano, T. Yokoya, T. Takeuchi, T. Takahashi, T. Mochiku, K. Kadowaki, P. Guptasarma, and D. G. Hinks, *Nature* (London) **392**, 157 (1998).
- ⁷S. H. Pan, J. P. O'Neal, R. L. Badzey, C. Chamon, H. Ding, J. R. Engelbrecht, Z. Wang, H. Eisaki, S. Uchida, A. K. Gupta, K.-W. Ng, E. W. Hudson, K. M. Lang, and J. C. Davis, *Nature* (London) **413**, 282 (2001).
- ⁸K. K. Gomes, A. N. Pasupathy, A. Pushp, S. Ono, Y. Ando, and A. Yazdani, *Nature* (London) **447**, 569 (2007).
- ⁹T. Hanaguri, C. Lupien, Y. Kohsaka, D.-H. Lee, M. Azuma, M. Takano, H. Takagi, and J. C. Davis, *Nature* (London) **430**, 1001 (2004).
- ¹⁰A. Kaminski, J. Mesot, H. Fretwell, J. C. Campuzano, M. R. Norman, M. Randeria, H. Ding, T. Sato, T. Takahashi, T. Mochiku, K. Kadowaki, and H. Hoehst, *Phys. Rev. Lett.* **84**, 1788 (2000).
- ¹¹T. Valla, T. E. Kidd, W.-G. Yin, G. D. Gu, P. D. Johnson, Z.-H. Pan, and A. V. Fedorov, *Phys. Rev. Lett.* **98**, 167003 (2007).
- ¹²P. V. Bogdanov, A. Lanzara, S. A. Kellar, X. J. Zhou, E. D. Lu, W. J. Zheng, G. Gu, J.-I. Shimoyama, K. Kishio, H. Ikeda, R. Yoshizaki, Z. Hussain, and Z. X. Shen, *Phys. Rev. Lett.* **85**, 2581 (2000).
- ¹³A. Kaminski, M. Randeria, J. C. Campuzano, M. R. Norman, H. Fretwell, J. Mesot, T. Sato, T. Takahashi, and K. Kadowaki, *Phys. Rev. Lett.* **86**, 1070 (2001).
- ¹⁴A. Damascelli, Z. Hussain, and Z.-X. Shen, *Rev. Mod. Phys.* **75**, 473 (2003).
- ¹⁵J. C. Campuzano, M. R. Norman, and M. Randeria, in *The Physics of Superconductors*, edited by K. H. Bennemann and J. B. Ketterson (Springer, Berlin, 2004), Vol. 2, p. 167.
- ¹⁶A. Kordyuk, S. Borisenko, V. Zabolotnyy, R. Schuster, D. Inosov, R. Follath, A. Varykhalov, L. Patthey, and H. Berger, *Phys. Rev. B* **79**, 020504(R) (2009).
- ¹⁷H. Ding, M. R. Norman, T. Yokoya, T. Takeuchi, M. Randeria, J. C. Campuzano, T. Takahashi, T. Mochiku, and K. Kadowaki, *Phys. Rev. Lett.* **78**, 2628 (1997).
- ¹⁸P. Schwaller, T. Greber, P. Aebi, J. M. Singer, H. Berger, L. Forr, and J. Osterwalder, *Eur. Phys. J. B* **18**, 215 (2000).
- ¹⁹M. M. Halmann and M. Steinberg, *Greenhouse Gas Carbon Dioxide Migration* (CRC, Boca Raton, Florida, 1998), p. 47.
- ²⁰Y.-D. Chuang, A. D. Gromko, A. V. Fedorov, Y. Aiura, K. Oka, Y. Ando, M. Lindroos, R. S. Markiewicz, A. Bansil, and D. S. Dessau, *Phys. Rev. B* **69**, 094515 (2004).
- ²¹S. V. Borisenko, A. A. Kordyuk, S. Legner, T. K. Kim, M. Knupfer, C. M. Schneider, J. Fink, M. S. Golden, M. Sing, R. Claessen, A. Yaresko, H. Berger, C. Grazioli, and S. Turchini, *Phys. Rev. B* **69**, 224509 (2004).
- ²²S. V. Borisenko, A. A. Kordyuk, A. Koitzsch, J. Fink, J. Geck, V. Zabolotnyy, M. Knupfer, B. Büchner, H. Berger, M. Falub, M. Shi, J. Krempasky, and L. Patthey, *Phys. Rev. Lett.* **96**, 067001 (2006).
- ²³A. A. Kordyuk, S. V. Borisenko, A. N. Yaresko, S.-L. Drechsler, H. Rosner, T. K. Kim, A. Koitzsch, K. A. Nenkov, M. Knupfer, J. Fink, R. Follath, H. Berger, B. Keimer, S. Ono, and Y. Ando, *Phys. Rev. B* **70**, 214525 (2004).
- ²⁴T. Sato, T. Kamiyama, Y. Naitoh, T. Takahashi, I. Chong, T. Terashima, and M. Takano, *Phys. Rev. B* **63**, 132502 (2001).
- ²⁵M. Hashimoto, T. Yoshida, H. Yagi, M. Takizawa, A. Fujimori, M. Kubota, K. Ono, K. Tanaka, D. H. Lu, Z.-X. Shen, S. Ono, and Yoichi Ando, *Phys. Rev. B* **77**, 094516 (2008).